

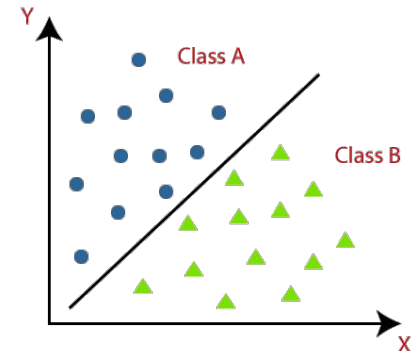
Vincent Naayem  
Supervised by:  
Prof. Alexandre Alahi

# Deep Learning for CT scans

Master Project

# Introduction

- How can we leverage the latest advancements in medical segmentation to develop an effective framework for delineating anatomical structures on CT scan images?
- Définitions:
  - CT scans
  - Deep Learning
  - Semantic Segmentation
- Terminology:
  - Class: An organ
  - Annotations: Annotations of this organ in many scans



# Introduction CT scans

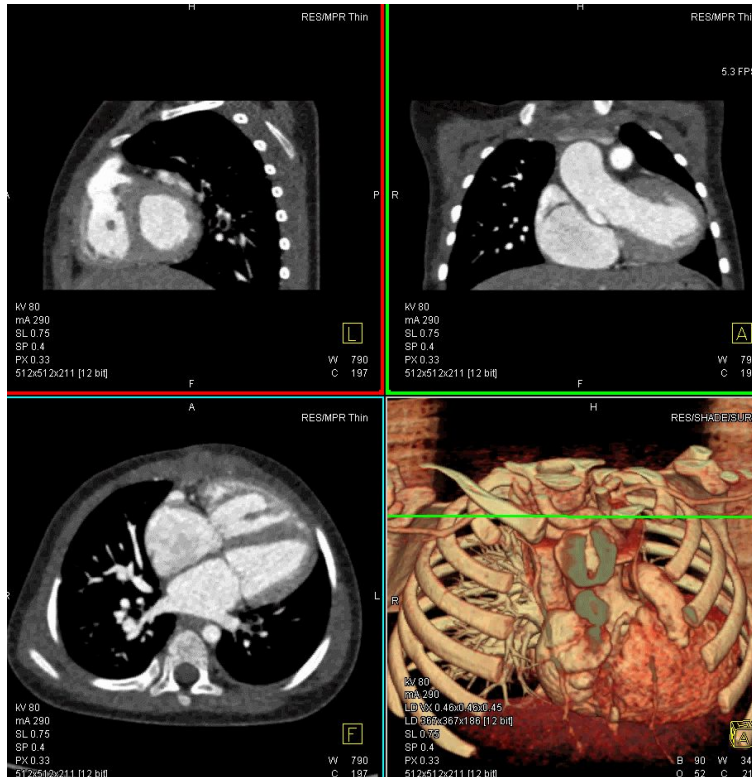
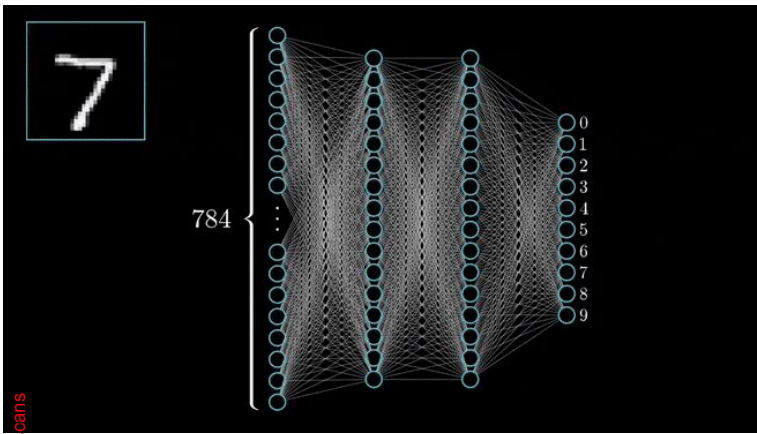


Image source: Korean Journal of Radiology

# Introduction Deep Learning and Segmentation



■ Deep Learning for CT scans

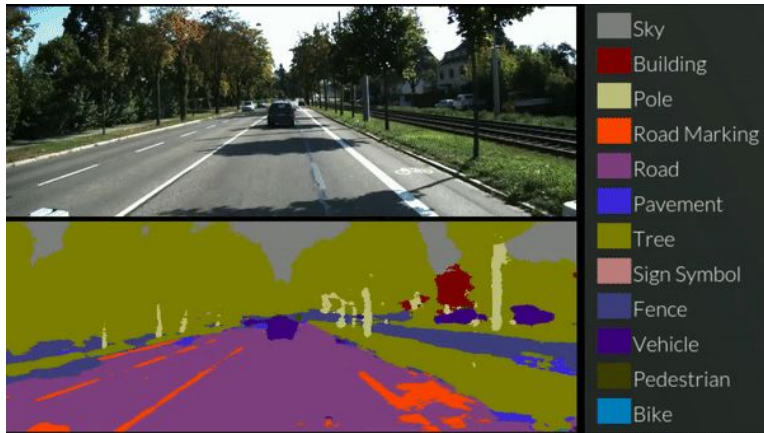
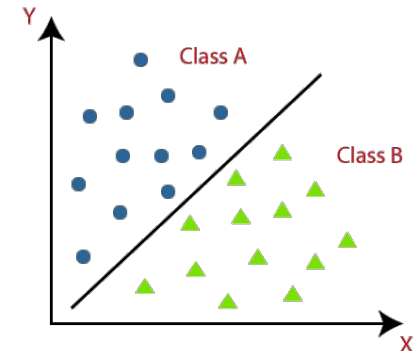


Image source: segmentation: <https://vladlen.info/>  
neural net: 3Blue1Brown

# Introduction

- How can we leverage the latest advancements in medical segmentation to develop an effective framework for delineating anatomical structures on CT scan images?
- Définitions:
  - CT scans
  - Deep Learning
  - Semantic Segmentation
- Terminology:
  - Class: An organ
  - Annotations: Annotations of this organ in many scans





# Drs requirements

Report of the meeting and keypoints

# Wishes

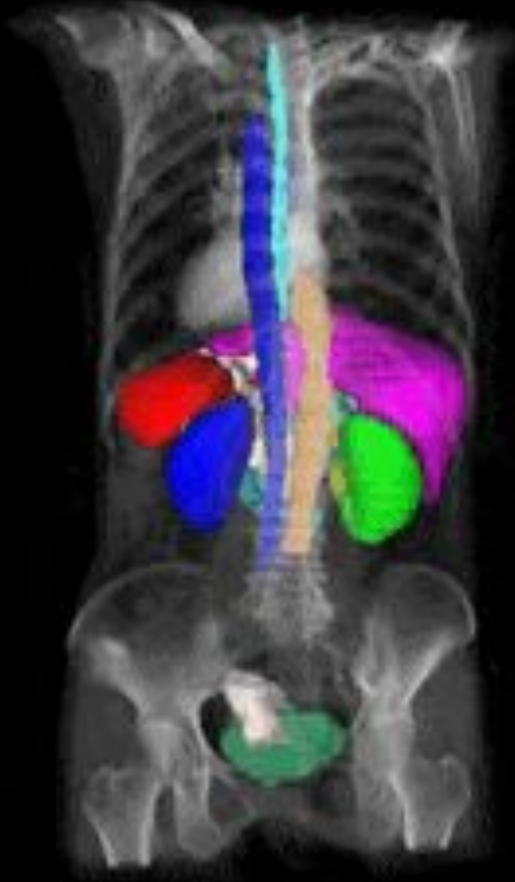
- Intuitive and easy-to-use interface designed specifically for radiologists and other healthcare professionals.
- Automated segmentation capabilities that can accurately identify and separate structures within CT scans, including organs and tumors, with minimal user input.
- Generates detailed automated reports based on CT scans, highlighting any abnormalities or potential issues for quick and efficient diagnosis.
- Annotated diagnoses with comprehensive explanations of the findings in the CT scan, providing valuable information for patient treatment and follow-up.
- Seamless integration of PET-CT imaging for more comprehensive analysis and diagnosis.
- Continuously updated with the latest advancements in deep learning algorithms and medical imaging, ensuring the product stays current and relevant.
- Advanced security measures to protect patient privacy and confidential medical data, ensuring compliance with relevant regulations.
- Vendor-agnostic compatibility, able to work seamlessly with all popular vendors such as GE and Siemens.
- Integrates with other medical systems and databases, allowing for easy data sharing and collaboration.
- Scalable architecture that can accommodate future growth and expansion, ensuring the product remains relevant and useful for years to come.

# Requirements

- Collect various datasets
- Compare state of the art solutions
- Assess promising methods for improving on state of the art
- Run the best current solution
- Evaluate the relation between dataset size and model performance

# Plans

- Intro
- Definitions (DL, CT, Segmentation)
- Drs requirements
- Datasets
- Models
- Comparison
- Labs and collabs
- Learning curve experiment
- Roadmap
- Conclusion



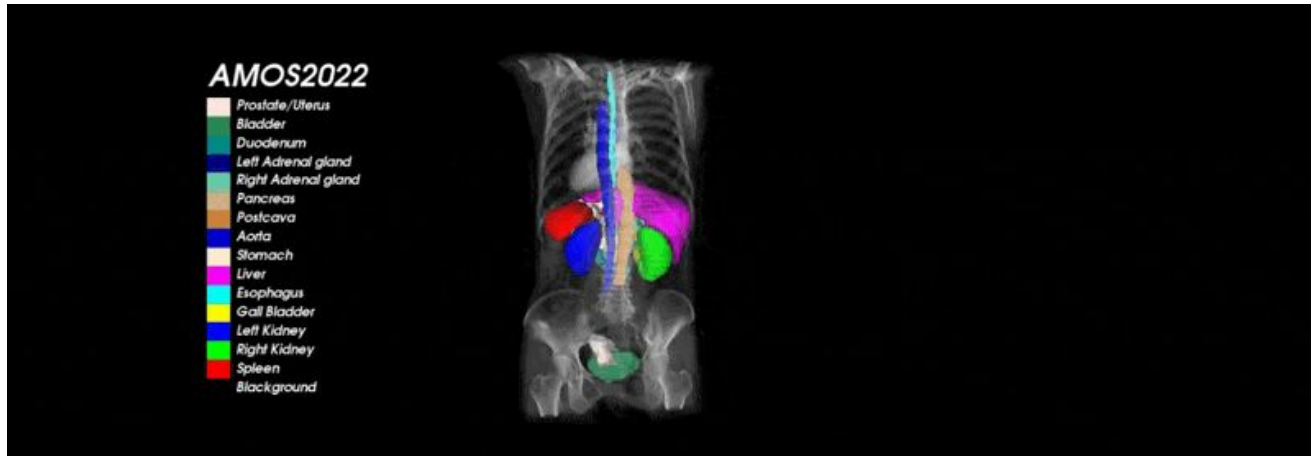
# Datasets

What are the datasets at our disposition? What data is available and how much data is it?

# Datasets

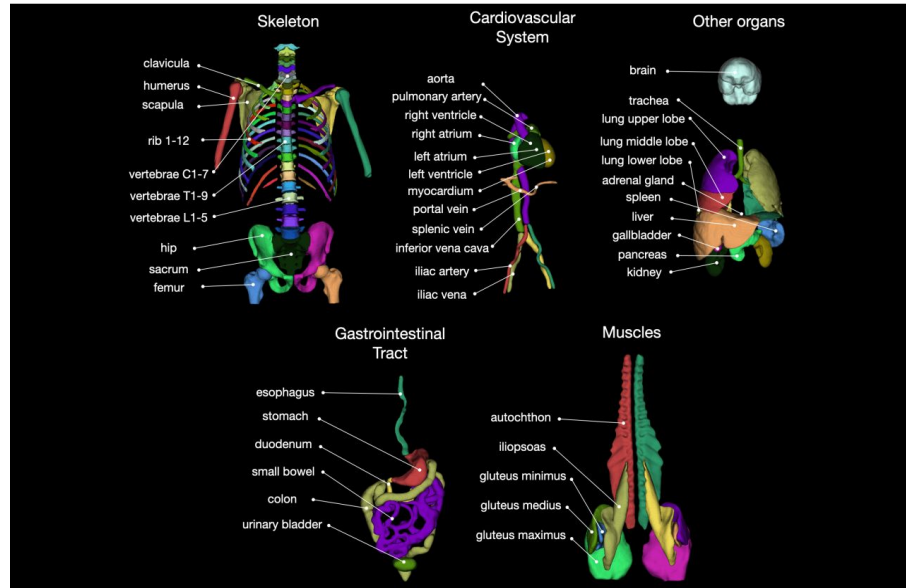
These datasets each combine delineations of many organs. Most frequent ones are major organs and abdominal structures. Combining many of them can help train generalizable models.

Levels of generalization: 1. patients, 2. scanners, 3. modalities



# Datasets

- 10 datasets available
- Total of 4000+ CT scans,
- 1000 from AbdomenCT-1K
- 1204 from Totalsegmentator
- 140 classes annotated total
- Biggest and newest dataset:
  - AMOS (500 CT scans, 15 organs classes)
  - Totalsegmentator (1204 CT scans, 104 organs classes)



Totalsegmentator  
(2022)

# Datasets

- Pixels:
  - 512x512
- axial slices:
  - 85 to 198
  - 148 to 241
  - 159 to 330
  - 42 to 1026
- In-plane resolution:
  - 0.54x0.54 mm
  - 0.98x0.98 mm
  - 1.27x1.27 mm
- Slice thickness:
  - 0.45 to 6 mm
  - 1.5 to 5mm
  - 2.5 to 3 mm
- Protocol
  - Portal venous
  - Contrast phase
  - full-bladder drinking protocol
  - Native
  - dual energy
- Countries: 10 +
- Annotators:
  - Radiologist (xp 3y, 5y)
  - Oncologist(xp 7y, 20y)
  - Agreement
- Scanners:
  - Aquillon, Brilliance, Phillips secura, Optima C, etc..
- Software:
  - MIPAV, ElastiX, ITKSNAP, Nora

# Datasets

TABLE 2.3: Number of samples per annotated organ in our database

| Organ                  | Value |
|------------------------|-------|
| Adrenal gland (L)      | 1904  |
| Adrenal gland (R)      | 1904  |
| Aorta                  | 1754  |
| Autochthon (L)         | 1204  |
| Autochthon (R)         | 1204  |
| Bladder                | 690   |
| Bones                  | 140   |
| Brain                  | 1375  |
| Brainstem              | 31    |
| Clavicula (L)          | 1204  |
| Clavicula (R)          | 1204  |
| Cochlea (L)            | 31    |
| Cochlea (R)            | 31    |
| Colon                  | 1354  |
| Colon cancer primaries | 126   |
| Duodenum               | 1854  |
| Esophagus              | 1904  |
| Face                   | 1204  |
| Femur (L)              | 1204  |
| Femur (R)              | 1204  |
| Gallbladder            | 1904  |
| Gluteus maximus (L)    | 1204  |
| Gluteus maximus (R)    | 1204  |
| Gluteus medius (L)     | 1204  |
| Gluteus medius (R)     | 1204  |
| Gluteus minimus (L)    | 1204  |
| Gluteus minimus (R)    | 1204  |
| Head of Femur (L)      | 150   |
| Head of Femur (R)      | 150   |
| Heart atrium (L)       | 1204  |
| Heart atrium (R)       | 1204  |
| Heart myocardium       | 1204  |
| Heart ventricle (L)    | 1204  |
| Heart ventricle (R)    | 1204  |
| hepatic tumor          | 303   |
| hepatic vessel         | 303   |
| Hip (L)                | 1204  |
| Hip (R)                | 1204  |
| Humerus (L)            | 1204  |
| Humerus (R)            | 1204  |
| Iliac artery (L)       | 1204  |
| Iliac artery (R)       | 1204  |
| Iliac vena (L)         | 1204  |
| Iliac vena (R)         | 1204  |
| Iliopsoas (L)          | 1204  |

| Organ                        | Value |
|------------------------------|-------|
| Iliopsoas (R)                | 1204  |
| Inferior vena cava           | 1774  |
| Intestine                    | 150   |
| Kidney (L)                   | 3084  |
| Kidney (R)                   | 3084  |
| Lacrimal gland (L)           | 31    |
| Lacrimal gland (R)           | 31    |
| Lens (L)                     | 31    |
| Lens (R)                     | 31    |
| Liver                        | 3215  |
| Liver Segments               | 50    |
| Liver tumor                  | 232   |
| Lung                         | 140   |
| Lung (L)                     | 31    |
| Lung (R)                     | 31    |
| Lung tumor                   | 64    |
| Lung lower lobe (L)          | 1204  |
| Lung lower lobe (R)          | 1204  |
| Lung middle lobe (R)         | 1204  |
| Lung upper lobe (L)          | 1204  |
| Lung upper lobe (R)          | 1204  |
| Mandible                     | 31    |
| Optic nerve (R)              | 31    |
| Optic nerve (L)              | 31    |
| Orbit (L)                    | 31    |
| Orbit (R)                    | 31    |
| Pancreas                     | 3186  |
| Pancreatic tumor mass        | 282   |
| Parotid gland (L)            | 31    |
| Parotid gland (R)            | 31    |
| Portal vein and splenic vein | 1754  |
| Prostate                     | 500   |
| Pulmonary artery             | 1204  |
| Rectum                       | 200   |
| Rib (L) 1                    | 1204  |
| Rib (L) 2                    | 1204  |
| Rib (L) 3                    | 1204  |
| Rib (L) 4                    | 1204  |
| Rib (L) 5                    | 1204  |
| Rib (L) 6                    | 1204  |
| Rib (L) 7                    | 1204  |
| Rib (L) 8                    | 1204  |
| Rib (L) 9                    | 1204  |
| Rib (L) 10                   | 1204  |
| Rib (L) 11                   | 1204  |
| Rib (L) 12                   | 1204  |
| Rib (R) 1                    | 1204  |
| Rib (R) 2                    | 1204  |
| Rib (R) 3                    | 1204  |
| Rib (R) 4                    | 1204  |

| Organ                   | Value |
|-------------------------|-------|
| Rib (R) 5               | 1204  |
| Rib (R) 6               | 1204  |
| Rib (R) 7               | 1204  |
| Rib (R) 8               | 1204  |
| Rib (R) 9               | 1204  |
| Rib (R) 10              | 1204  |
| Rib (R) 11              | 1204  |
| Rib (R) 12              | 1204  |
| Sacrum                  | 1204  |
| Scapula (L)             | 1204  |
| Scapula (R)             | 1204  |
| Small bowel             | 1254  |
| Spinal canal            | 31    |
| Spinal cord             | 31    |
| Spleen                  | 2985  |
| Stomach                 | 1904  |
| Submandibular gland (L) | 31    |
| Submandibular gland (R) | 31    |
| Trachea                 | 1204  |
| Urinary bladder         | 1204  |
| Uterus                  | 550   |
| Vertebrae C1            | 1204  |
| Vertebrae C2            | 1204  |
| Vertebrae C3            | 1204  |
| Vertebrae C4            | 1204  |
| Vertebrae C5            | 1204  |
| Vertebrae C6            | 1204  |
| Vertebrae C7            | 1204  |
| Vertebrae L1            | 1204  |
| Vertebrae L2            | 1204  |
| Vertebrae L3            | 1204  |
| Vertebrae L4            | 1204  |
| Vertebrae L5            | 1204  |
| Vertebrae T1            | 1204  |
| Vertebrae T10           | 1204  |
| Vertebrae T11           | 1204  |
| Vertebrae T12           | 1204  |
| Vertebrae T2            | 1204  |
| Vertebrae T3            | 1204  |
| Vertebrae T4            | 1204  |
| Vertebrae T5            | 1204  |
| Vertebrae T6            | 1204  |
| Vertebrae T7            | 1204  |
| Vertebrae T8            | 1204  |
| Vertebrae T9            | 1204  |

End of Table

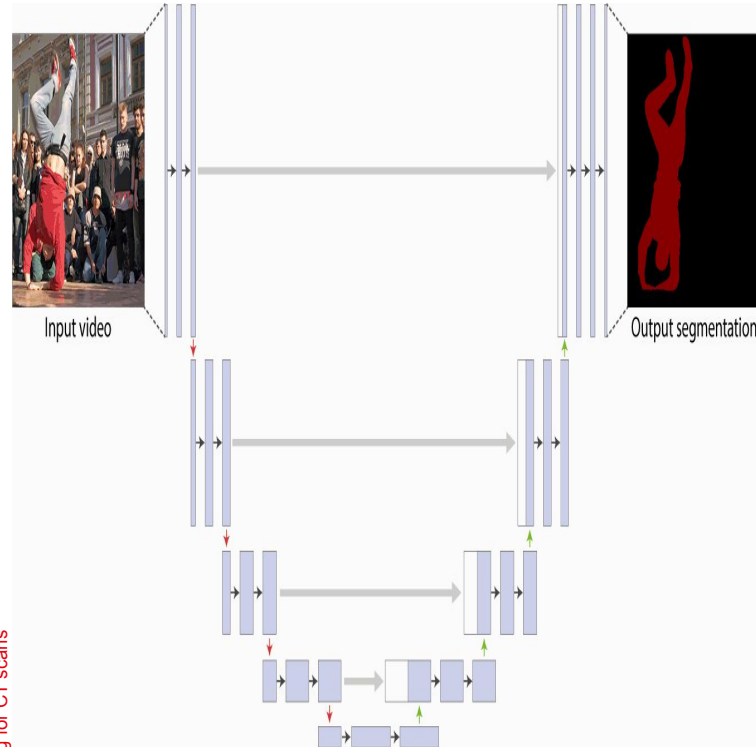
# Datasets

TABLE 2.4: Summary of the collected datasets and their contents.

| Dataset       | Organs   | # scans | Year | References   |
|---------------|--|---------|------|--|
| CT-ORG (LiTS) | Lung, Bones, Liver, Bladder, Kidney, Brain   | 140     | 2019 | Bilic et al., 2023   |
| Abdomen CT-1K | Spleen, Kidney, Liver, Pancreas  | 1000    | 2020 | Ma et al., 2021  |
| WORD          | Liver, Spleen, Kidney (L), Kidney (R), Stomach, Gallbladder, Esophagus, Pancreas, Duodenum, Colon, Intestine, Adrenal gland (L), Adrenal gland (R), Rectum, Head of Femur (L), Head of Femur (R)                     | 150     | 2021 | Luo et al., 2022   |
| BTCV Abdomen  | Liver, Spleen, Kidney (L), Kidney (R), Stomach, Gallbladder, Esophagus, Pancreas, Duodenum, Colon, Intestine, Adrenal gland (L), Adrenal gland (R), Rectum, Head of Femur (L), Head of Femur (R)                     | 50      | 2015 | <i>Multi-Atlas Labeling Beyond the Cranial Vault - Workshop and Challenge - syn3193805 - Wiki n.d.</i> |
| BTCV Cervix   | Bladder, uterus, Rectum, small bowel, Kidney (L)   | 50      | 2015 |  |
| AMOS          | Spleen, Kidney (R), Kidney (L), Gallbladder, Esophagus, Liver, Stomach, Aorta, Inferior vena cava, Pancreas, Adrenal gland (R), Adrenal gland (L), Duodenum, Bladder, Prostate, Uterus, Portal vein and splenic vein | 500     | 2022 | Ji et al., 2022  |
| CHAOS         | Liver  | 20      | 2021 | 2021   |
| TCIA T&V      | Brain, Lung, Mandible, Optic nerve, Orbit, Parotid gland, Spinal canal, Spinal cord, Submandibular gland, Cochlea, Lacrimal gland, Lens  | 31      | 2021 | <i>TCIA Test &amp; Validation Radiotherapy CT Planning Scan Dataset 2022</i>                           |
| MSD Liver     | Liver, Liver tumor   | 131     | 2018 | <i>The Medical Segmentation Decathlon 1 Nature Communications n.d.</i>                                 |
| MSD Lung      | Lung tumor   | 64      | 2018 |  |
| MSD Pancreas  | Pancreas, Tumor mass   | 282     | 2018 |  |

| Continuation of Table 2.4 |  |         |      |                           |
|---------------------------|--|---------|------|---------------------------|
| Dataset                   | Organs   | # scans | Year | References                |
| MSD Colon                 | Colon cancer primaries   | 226     | 2018 |                           |
| MSD Hepatic Vessels       | Hepatic tumor, Hepatic vessel  | 303     | 2018 |                           |
| MSD Spleen                | Spleen   | 41      | 2018 |                           |
| Total-segmentor           | adrenal gland left , adrenal gland right , aorta , autochthon left , autochthon right , brain , clavicular left , clavicular right , colon , duodenum , esophagus , face , femur left , femur right , gallbladder , gluteus maximus left , gluteus maximus right , gluteus medius left , gluteus medius right , gluteus minimus left , gluteus minimus right , heart atrium left , heart atrium right , heart myocardium , heart ventricle left , heart ventricle right , hip left , hip right , humerus left , humerus right , iliac artery left , iliac artery right , iliac vena left , iliac vena right , iliopsoas left , iliopsoas right , inferior vena cava , kidney left , kidney right , liver , lung lower lobe left , lung lower lobe right , lung middle lobe right , lung upper lobe left , lung upper lobe right , pancreas , portal vein and splenic vein , pulmonary artery , rib left 1 , rib left 10 , rib left 11 , rib left 12 , rib left 2 , rib left 3 , rib left 4 , rib left 5 , rib left 6 , rib left 7 , rib left 8 , rib left 9 , rib right 1 , rib right 10 , rib right 11 , rib right 12 , rib right 2 , rib right 3 , rib right 4 , rib right 5 , rib right 6 , rib right 7 , rib right 8 , rib right 9 , sacrum , scapula left , scapula right , small bowel , spleen , stomach , trachea , urinary bladder , vertebrae C1 , vertebrae C2 , vertebrae C3 , vertebrae C4 , vertebrae C5 , vertebrae C6 , vertebrae C7 , vertebrae L1 , vertebrae L2 , vertebrae L3 , vertebrae L4 , vertebrae L5 , vertebrae T1 , vertebrae T10 , vertebrae T11 , vertebrae T12 , vertebrae T2 , vertebrae T3 , vertebrae T4 , vertebrae T5 , vertebrae T6 , vertebrae T7 , vertebrae T8 , vertebrae T9 | 1204    | 2022 | (Wasserthal et al., 2022) |
| MedSeg LS                 | Liver segment 1, Liver segment 2, Liver segment 3, Liver segment 4, Liver segment 5, Liver segment 6, Liver segment 7, Liver segment 8   | 50      | 2021 | <i>Database n.d.</i>      |
| MedSeg IVC                | Inferior vena cava   | 20      | 2021 | <i>Database n.d.</i>      |

End of Table



■ Deep Learning for CT scans

# State-of-the-Art

What are the state-of-the-art models?  
What are their performance?

U-net architectures are the most common in medical image segmentation papers. It is a straightforward and flexible architecture performing well with small amount of data. Many variations exist and are SOTA.

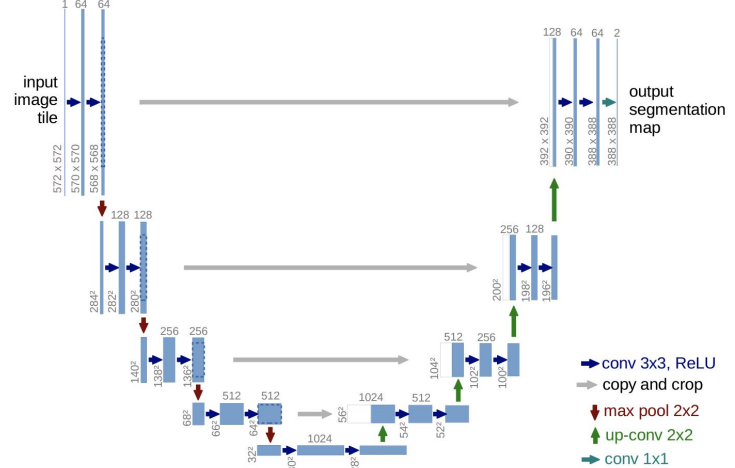


**Fig. 1.** U-net architecture (example for 32x32 pixels in the lowest resolution). Each blue box corresponds to a multi-channel feature map. The number of channels is denoted on top of the box. The x-y-size is provided at the lower left edge of the box. White boxes represent copied feature maps. The arrows denote the different operations.

# Introduction U-Net

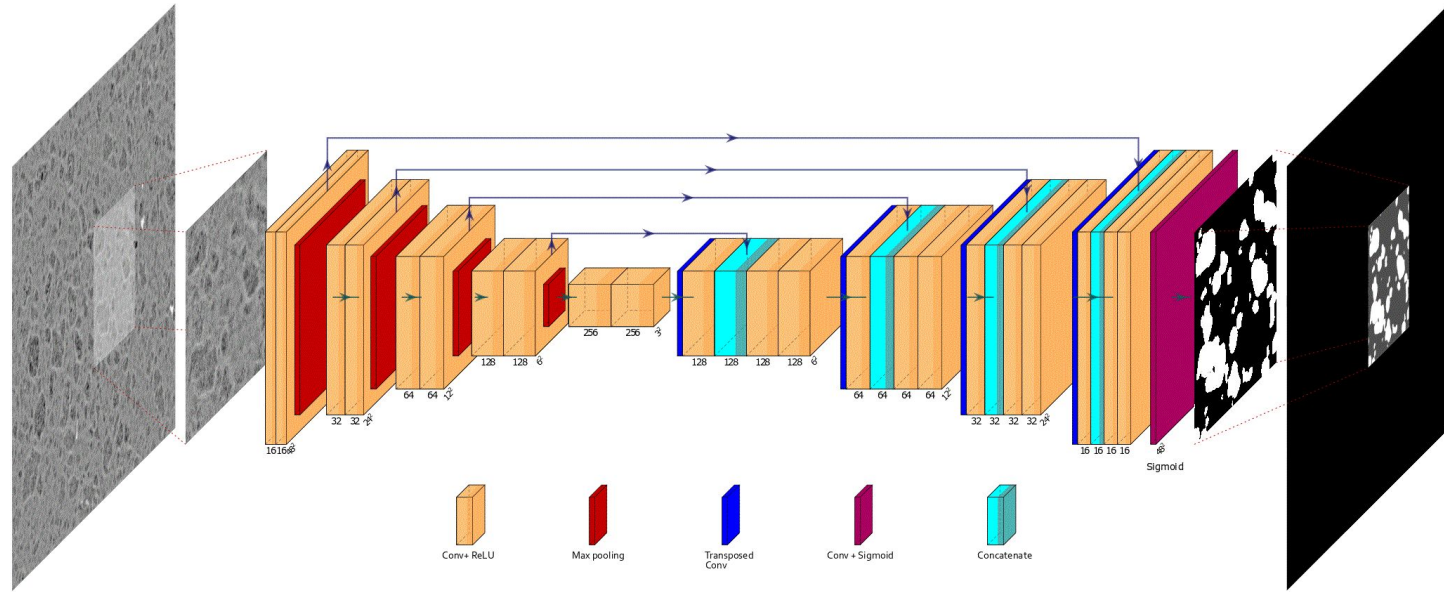


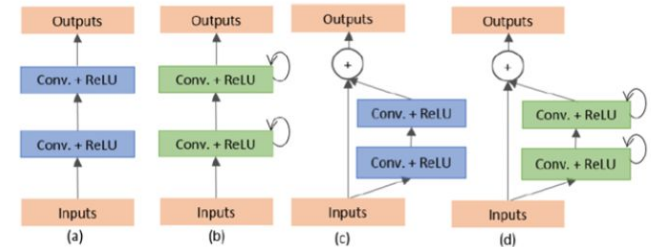
Image source: ifpennergiesnouvelles.com

# U-net Variations

U-net variations using different variants of convolutional units.

Fig 1: (a) Forward; (b) Recurrent; (c) Residual; (d) Recurrent Residual; convolutional units

- 3D U-net
- Attention U-net
- Residual U-Net
- Recurrent Convolutional Network
- Dense U-net
- U-net++
- Adversarial U-net
- Cascaded arrangement



Vincent

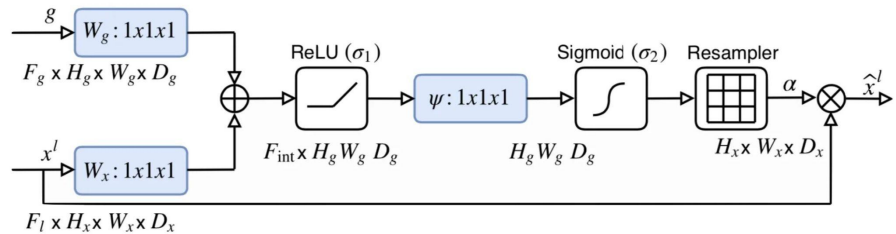
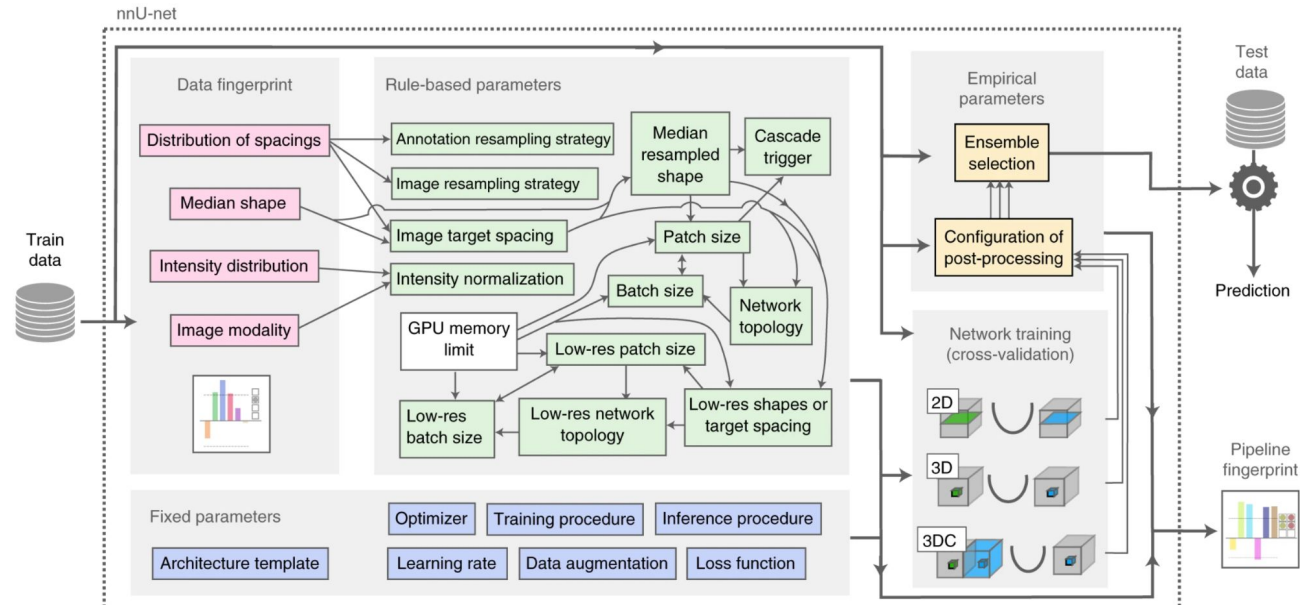


Fig 2: Attention Gates

# Framework: nnU-net

nnU-Net surpasses most specialised deep learning pipelines in 19 public international competitions and sets a new state of the art in the majority of the 49 tasks.

Publicly available  
Open-source tool  
Pytorch



# Swin UNETR

- (Hatamizadeh et al., 2022) Nvidia
- Self-supervised learning
- Combine (ViT)s with U-Net architecture

Fig 1  
self-supervised learning  
of swin UNETR

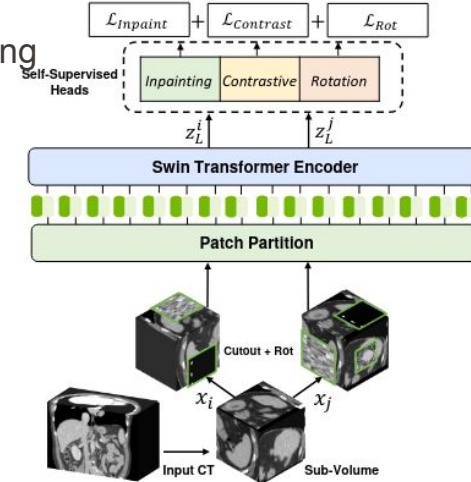
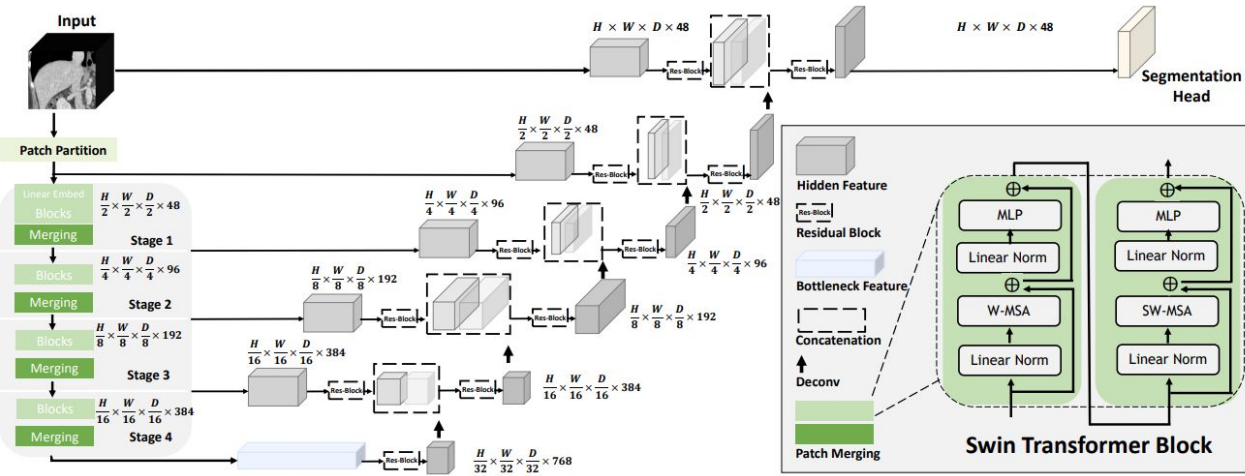


Fig 2  
Architecture of  
swin UNETR





# Results

We gathered results from competitive research. We replicated these results in-house training a model from scratch with some available data.

# Metrics

The metrics mostly used are:

DSC, the dice score coefficient

& IoU, Intersection over Union also called Jaccard index

They are very similar, always positively correlated

$$J(A, B) = \frac{|A \cap B|}{|A \cup B|} \quad DSC = \frac{2|X \cap Y|}{|X| + |Y|}$$

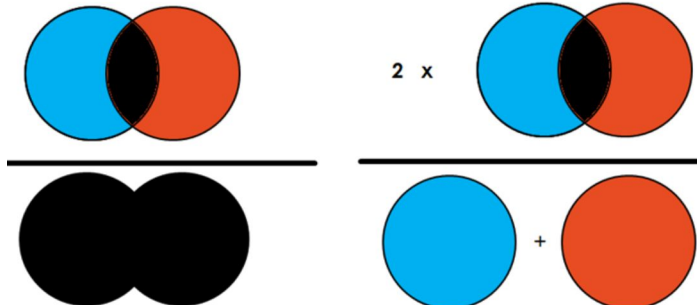
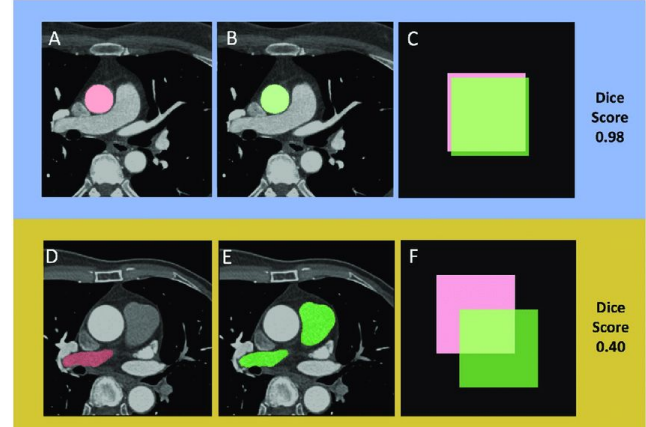


Illustration of IoU and Dice Coefficient.



Dice score visualization. The Dice score is used to gauge model performance, ranging from 0 to 1. 1 corresponds to a pixel perfect match between the deep learning model output (red, A and D) and ground truth annotation (green, B and D). The model output with the higher Dice score (A) had greater overlap (C) with the ground truth (B) than the output (D) that had lesser overlap (F), as it did not predict that main pulmonary artery that was annotated in (E). <https://doi.org/10.1371/journal.pone.0232573.g002>

# State-of-the-art results

Some studies (WORD paper) underlines that segmentation is solved for major and bigger organs

Smaller organs or organs with more variations can remain challenging.

6

Luo *et al.*/Medical Image Analysis (2022)

| Method            | nnUNet(2D)  | nnUNetV2(2D)      | ResUNet(2D)       | DeepLabV3+(2D) | UNet++(2D)  | AttUNet(3D) | nnUNet(3D)         | nnUNetV2(3D)      | UNETR(3D)   | CoTr(3D)    |
|-------------------|-------------|-------------------|-------------------|----------------|-------------|-------------|--------------------|-------------------|-------------|-------------|
| Liver             | 95.38±4.45  | 96.19±2.16        | 96.55±0.89        | 96.21±1.34     | 96.33±1.40  | 96.00±1.01  | 96.45±0.85         | <b>96.59±6.10</b> | 94.67±1.92  | 95.58±1.59  |
| Spleen            | 93.33±11.85 | 94.33±7.72        | 95.26±2.84        | 94.68±5.64     | 94.64±4.22  | 94.90±1.63  | 95.98±0.89         | <b>96.09±8.10</b> | 92.85±3.03  | 94.9±1.37   |
| Kidney (L)        | 90.05±19.35 | 91.29±18.15       | 95.63±1.20        | 92.01±13.00    | 93.36±5.06  | 94.65±1.38  | 95.40±0.95         | <b>95.63±9.20</b> | 91.49±5.81  | 93.26±3.07  |
| Kidney (R)        | 89.86±19.56 | 91.20±17.22       | 95.84±1.16        | 91.84±14.41    | 93.34±7.38  | 94.7±2.78   | 95.68±1.07         | <b>95.83±9.00</b> | 91.72±7.06  | 93.63±3.01  |
| Stomach           | 89.97±4.96  | 91.12±3.60        | 91.58±2.86        | 91.16±3.07     | 91.33±3.13  | 91.15±2.74  | <b>91.69±2.5</b>   | 91.57±3.05        | 85.56±6.12  | 89.99±4.49  |
| Gallbladder       | 78.43±16.48 | 83.19±12.22       | 82.83±11.8        | 80.05±17.92    | 81.21±12.24 | 81.38±10.95 | 83.19±8.81         | <b>83.72±8.19</b> | 65.08±19.63 | 76.4±16.48  |
| Esophagus         | 78.08±13.99 | 77.79±13.51       | 77.17±14.68       | 74.88±14.69    | 78.36±12.84 | 76.87±15.12 | <b>78.51±12.22</b> | 77.36±13.66       | 67.71±13.46 | 74.37±14.92 |
| Pancreas          | 82.33±6.5   | 83.55±5.87        | 83.56±5.60        | 82.39±6.68     | 84.43±6.77  | 83.55±6.2   | <b>85.04±5.78</b>  | 85.00±5.95        | 74.79±9.31  | 81.02±7.23  |
| Duodenum          | 63.47±15.81 | 64.47±15.87       | 66.67±15.36       | 62.81±15.21    | 65.99±15.79 | 67.68±14.01 | <b>68.31±16.29</b> | 67.73±16.75       | 57.56±11.23 | 63.58±14.88 |
| Colon             | 83.06±8.32  | 83.92±8.45        | 83.57±8.69        | 82.72±8.79     | 83.22±8.98  | 85.72±8.50  | <b>87.41±7.38</b>  | 87.26±8.25        | 74.62±11.5  | 84.14±7.82  |
| Intestine         | 85.6±4.08   | 86.83±4.02        | 86.76±3.56        | 85.96±4.02     | 86.37±4.01  | 88.19±3.34  | 89.3±2.75          | <b>89.37±3.11</b> | 80.4±4.59   | 86.39±3.51  |
| Adrenal           | 69.9±11.07  | 70.0±11.86        | 70.9±10.12        | 66.82±10.81    | 71.04±10.65 | 70.23±9.31  | 72.38±8.98         | <b>72.98±8.09</b> | 60.76±8.32  | 69.06±9.26  |
| Rectum            | 81.66±6.64  | 81.49±7.37        | 82.16±6.73        | 81.85±6.67     | 81.44±6.7   | 80.47±5.44  | <b>82.41±4.9</b>   | 82.32±5.26        | 74.06±8.03  | 80.0±5.4    |
| Bladder           | 90.49±14.73 | 90.15±16.85       | 91.0±13.5         | 90.86±14.07    | 92.09±11.53 | 89.71±15.00 | <b>92.59±8.27</b>  | 92.11±9.75        | 85.42±18.17 | 89.27±18.28 |
| Head of Femur (L) | 93.28±5.31  | 93.28±5.12        | <b>93.39±5.11</b> | 92.01±4.76     | 93.38±5.12  | 91.90±4.39  | 91.99±4.72         | 92.56±4.19        | 89.47±6.4   | 91.03±4.81  |
| Head of Femur (R) | 93.78±4.38  | <b>93.93±4.29</b> | 93.88±4.30        | 92.29±4.01     | 93.88±4.21  | 92.43±3.68  | 92.74±3.63         | 92.49±4.03        | 90.17±4.0   | 91.87±3.32  |
| Mean              | 84.92±5.39  | 85.80±5.27        | 86.67±4.81        | 84.91±5.05     | 86.28±3.96  | 86.21±4.78  | <b>87.44±4.33</b>  | 87.41±4.57        | 79.77±4.92  | 84.66±5.45  |

Table 4. Performance comparison (DSC (%)) of 16 abdominal organs segmentation using ten recent segmentation methods.

# State-of-the-art results

Some studies (WORD paper) underlines that segmentation is solved for major and bigger organs

Smaller organs or organs with more variations can remain challenging.

6

Luo *et al.* / Medical Image Analysis (2022)

| Method            | nnUNet(2D)  | nnUNetV2(2D)      | ResUNet(2D)       | DeepLabV3+(2D) | UNet++(2D)  | AttUNet(3D) | nnUNet(3D)         | nnUNetV2(3D)      | UNETR(3D)   | CoTr(3D)    |
|-------------------|-------------|-------------------|-------------------|----------------|-------------|-------------|--------------------|-------------------|-------------|-------------|
| Liver             | 95.38±4.45  | 96.19±2.16        | 96.55±0.89        | 96.21±1.34     | 96.33±1.40  | 96.00±1.01  | 96.45±0.85         | <b>96.59±6.10</b> | 94.67±1.92  | 95.58±1.59  |
| Spleen            | 93.33±11.85 | 94.33±7.72        | 95.26±2.84        | 94.68±5.64     | 94.64±4.22  | 94.90±1.63  | 95.98±0.89         | <b>96.09±8.10</b> | 92.85±3.03  | 94.9±1.37   |
| Kidney (L)        | 90.05±19.35 | 91.29±18.15       | 95.63±1.20        | 92.01±13.00    | 93.36±5.06  | 94.65±1.38  | 95.40±0.95         | <b>95.63±9.20</b> | 91.49±5.81  | 93.26±3.07  |
| Kidney (R)        | 89.86±19.56 | 91.20±17.22       | 95.84±1.16        | 91.84±14.41    | 93.34±7.38  | 94.7±2.78   | 95.68±1.07         | <b>95.83±9.00</b> | 91.72±7.06  | 93.63±3.01  |
| Stomach           | 89.97±4.96  | 91.12±3.60        | 91.58±2.86        | 91.16±3.07     | 91.33±3.13  | 91.15±2.74  | <b>91.69±2.5</b>   | 91.57±3.05        | 85.56±6.12  | 89.99±4.49  |
| Gallbladder       | 78.43±16.48 | 83.19±12.22       | 82.83±11.8        | 80.05±17.92    | 81.21±12.24 | 81.38±10.95 | 83.19±8.81         | <b>83.72±8.19</b> | 65.08±19.63 | 76.4±16.48  |
| Esophagus         | 78.08±13.99 | 77.79±13.51       | 77.17±14.68       | 74.88±14.69    | 78.36±12.84 | 76.87±15.12 | <b>78.51±12.22</b> | 77.36±13.66       | 67.71±13.46 | 74.37±14.92 |
| Pancreas          | 82.33±6.5   | 83.55±5.87        | 83.56±5.60        | 82.39±6.68     | 84.43±6.77  | 83.55±6.2   | <b>85.04±5.78</b>  | 85.00±5.95        | 74.79±9.31  | 81.02±7.23  |
| Duodenum          | 63.47±15.81 | 64.47±15.87       | 66.67±15.36       | 62.81±15.21    | 65.99±15.79 | 67.68±14.01 | <b>68.31±16.29</b> | 67.73±16.75       | 57.56±11.23 | 63.58±14.88 |
| Colon             | 83.06±8.32  | 83.92±8.45        | 83.57±8.69        | 82.72±8.79     | 83.22±8.98  | 85.72±8.50  | <b>87.41±7.38</b>  | 87.26±8.25        | 74.62±11.5  | 84.14±7.82  |
| Intestine         | 85.6±4.08   | 86.83±4.02        | 86.76±3.56        | 85.96±4.02     | 86.37±4.01  | 88.19±3.34  | 89.3±2.75          | <b>89.37±3.11</b> | 80.4±4.59   | 86.39±3.51  |
| Adrenal           | 69.9±11.07  | 70.0±11.86        | 70.9±10.12        | 66.82±10.81    | 71.04±10.65 | 70.23±9.31  | 72.38±8.98         | <b>72.98±8.09</b> | 60.76±8.32  | 69.06±9.26  |
| Rectum            | 81.66±6.64  | 81.49±7.37        | 82.16±6.73        | 81.85±6.67     | 81.44±6.7   | 80.47±5.44  | <b>82.41±4.9</b>   | 82.32±5.26        | 74.06±8.03  | 80.0±5.4    |
| Bladder           | 90.49±14.73 | 90.15±16.85       | 91.0±13.5         | 90.86±14.07    | 92.09±11.53 | 89.71±15.00 | <b>92.59±8.27</b>  | 92.11±9.75        | 85.42±18.17 | 89.27±18.28 |
| Head of Femur (L) | 93.28±5.31  | 93.28±5.12        | <b>93.39±5.11</b> | 92.01±4.76     | 93.38±5.12  | 91.90±4.39  | 91.99±4.72         | 92.56±4.19        | 89.47±6.4   | 91.03±4.81  |
| Head of Femur (R) | 93.78±4.38  | <b>93.93±4.29</b> | 93.88±4.30        | 92.29±4.01     | 93.88±4.21  | 92.43±3.68  | 92.74±3.63         | 92.49±4.03        | 90.17±4.0   | 91.87±3.32  |
| Mean              | 84.92±5.39  | 85.80±5.27        | 86.67±4.81        | 84.91±5.05     | 86.28±3.96  | 86.21±4.78  | <b>87.44±4.33</b>  | 87.41±4.57        | 79.77±4.92  | 84.66±5.45  |

Table 4. Performance comparison (DSC (%)) of 16 abdominal organs segmentation using ten recent segmentation methods.

|            |  |
|------------|--|
| Vincent    |  |
| Swin UNETR |  |
| 0.96       |  |
| 0.948      |  |
| 0.95       |  |
| 0.95       |  |
| 0.91       |  |
| 0.65       |  |
| 0.75       |  |
| 0.81       |  |
| 0.64       |  |
| 0.83       |  |
| 0.855      |  |
| 0.686      |  |
| 0.769      |  |
| 0.914      |  |
| 0.90       |  |
| 0.895      |  |
| 0.84       |  |

# State-of-the-art results

AMOS benchmark results published in 2022

| Model       | Mean DSC | Spleen | Right kidney | Left kidney | Gallbladder | Esophagus | Liver | Stomach | Aorta | Postcava | Pancreas | Right adrenal gland | Left adrenal gland | Duodenum | Bladder | Prostate/Uterus |
|-------------|----------|--------|--------------|-------------|-------------|-----------|-------|---------|-------|----------|----------|---------------------|--------------------|----------|---------|-----------------|
| nnUNet      | 90.0%    | 97.1%  | 96.4%        | 96.2%       | 83.2%       | 87.5%     | 97.6% | 92.2%   | 96.0% | 92.5%    | 88.6%    | 81.2%               | 81.7%              | 85.0%    | 90.5%   | 85.0%           |
| Swin-UNITER | 86.4%    | 95.5%  | 93.8%        | 94.5%       | 77.3%       | 83.0%     | 95.9% | 88.9%   | 94.7% | 89.6%    | 84.9%    | 77.2%               | 78.3%              | 78.6%    | 85.8%   | 77.4%           |
| nnFormer    | 85.6%    | 95.9%  | 93.5%        | 94.8%       | 78.5%       | 81.1%     | 95.9% | 89.4%   | 94.2% | 88.3%    | 85.0%    | 75.0%               | 75.9%              | 78.4%    | 83.9%   | 74.6%           |
| VNet        | 82.0%    | 94.2%  | 91.9%        | 92.6%       | 70.2%       | 79.0%     | 94.7% | 84.8%   | 93.0% | 87.4%    | 80.5%    | 72.6%               | 73.2%              | 71.7%    | 77.0%   | 66.6%           |
| UNTER       | 78.3%    | 92.7%  | 88.5%        | 90.6%       | 66.5%       | 73.3%     | 94.1% | 78.7%   | 91.4% | 84.0%    | 74.5%    | 68.1%               | 65.3%              | 62.4%    | 77.4%   | 67.5%           |
| CoTr        | 77.1%    | 91.1%  | 87.2%        | 86.4%       | 60.5%       | 80.9%     | 91.6% | 80.1%   | 93.7% | 87.7%    | 76.3%    | 73.7%               | 71.7%              | 68.0%    | 67.4%   | 40.8%           |

# Inference with nnU-Net (ours)

We used nnU-net, the most complete framework for biomedical segmentation.  
We trained it with the WORD dataset.

Performance of our trained model (DSC(%)) of 16 abdominal organs segmentation:

■ Deep Learning for CT scans

| Organ | liver | spleen | left kidney | right kidney | stomach | gall/bladder | eso/phagus | pancreas | duodenum | colon | intestine | adrenal | rectum | bladder | Head of femur L | Head of femur R |
|-------|-------|--------|-------------|--------------|---------|--------------|------------|----------|----------|-------|-----------|---------|--------|---------|-----------------|-----------------|
| DSC % | 96.36 | 96.11  | 95.23       | 95.14        | 93.46   | 83.18        | 82.37      | 84.65    | 66.13    | 82.9  | 83.6      | 73.99   | 80.89  | 90.66   | 94.42           | 93.57           |

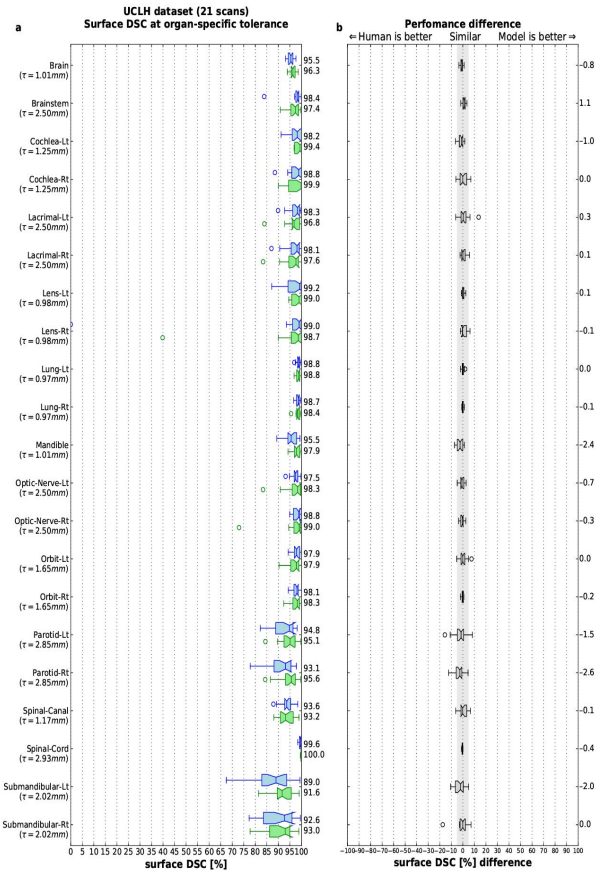
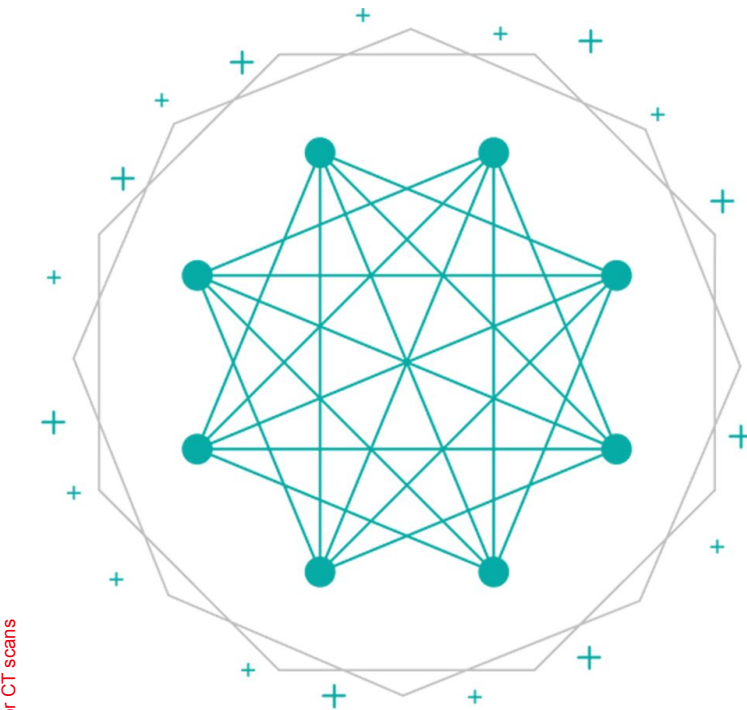


**Figure 4 | UCLH test set: Quantitative performance of the model in comparison to radiographers.** (a) The model achieves a surface DSC similar to humans in all 21 organs at risk (on the UCLH held out test set) when compared to the gold standard for each organ at an organ-specific tolerance  $\tau$ . Blue: our model, green: radiographers. (b) Performance difference between the model and the radiographers. Each blue dot represents a model-radiographer pair. The grey area highlights non-substantial differences (-5% to +5%).

The box extends from the lower to upper quartile values of the data, with a line at the median. The whiskers indicate most extreme, non-outlier data points. Where data lies outside 1.5 × interquartile range it is represented as a circular flier. The notches represent the 95% confidence interval (CI) around the median.

# State-of-the-art results

Following deepMind studies, in comparison to oncologists the model achieves similar performance as 4 years of experience radiologists.



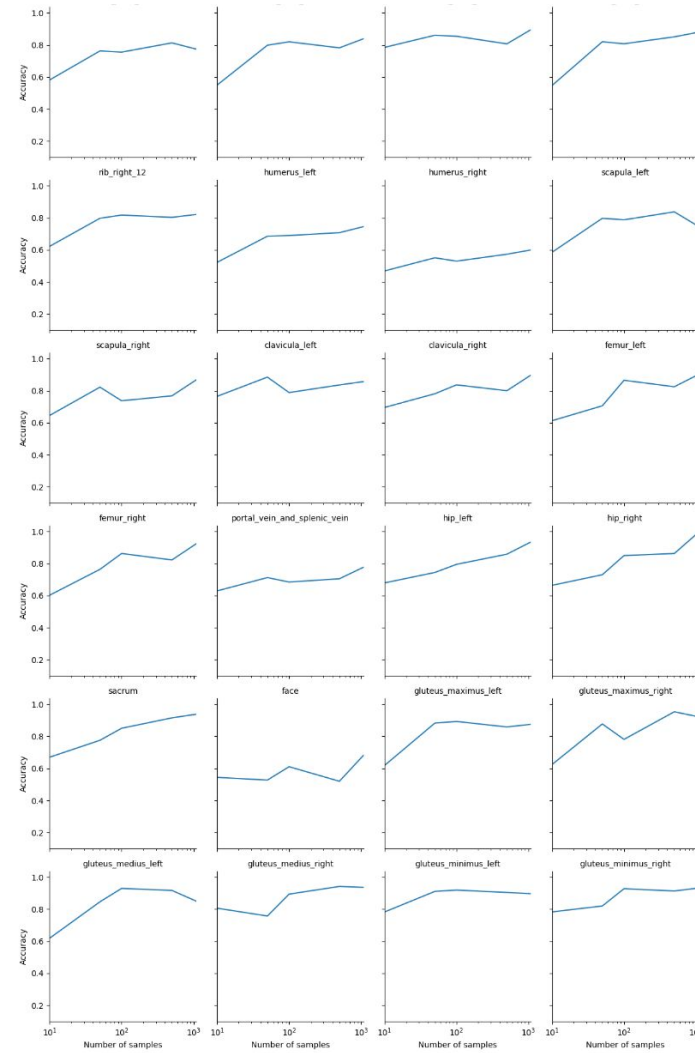
■ Deep Learning for CT scans

# Key contributors

The main contributors and collaborations

# About collaborations

- Authors of U-Net (Ronenburger, 2015); nnU-Net (Fabien Insee, 2018); Totalsegmentator (Wasserthal, 2022) and others all work now for DKFZ a german Laboratory.
- Project MONAI is a collaboration between NVIDIA and King's College London, DKFZ and plenty of hospitals and clinics.
- Focused on developing best practices for AI in healthcare imaging
- Flagship framework is MONAI Core, built on existing toolkits
- Advisory Board and nine working groups led by medical research community leaders
- Working groups focus on various aspects of the project, including imaging I/O, data ingestion, transformations, federated learning, evaluation, reproducibility, benchmarking, and deployment
- Ambitious effort to advance the field of AI in healthcare imaging.



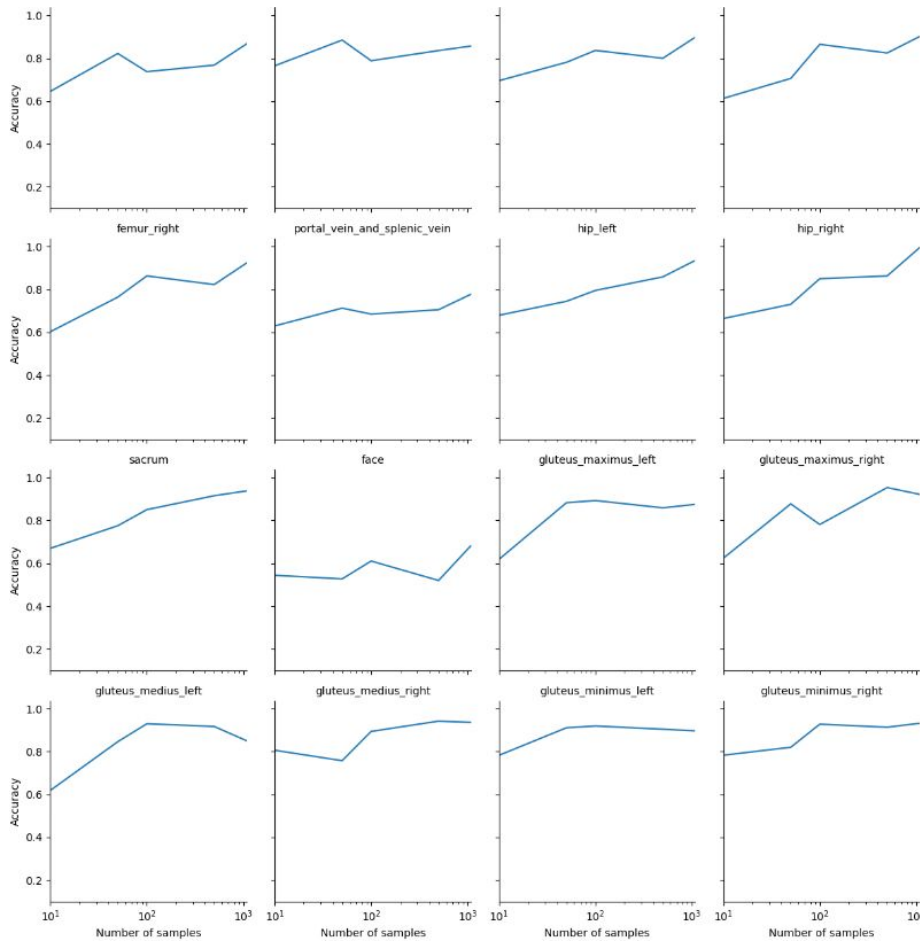
# Learning curve

How much data do we need to achieve satisfactory performances?

# Experiment

- Totalsegmentator dataset: 1204 images, 104 classes
  - nnU-Net performance over a large number of classes
  - Effects of # training images
1. Replicate the results of Totalsegmentator with nnU-Net
  2. Pre-train nnU-Net on WORD (100 images, 15 classes)
  3. Train 5 differents models on [10, 50, 100, 500, 1000] training images
    - Trainings are ran over 4000 epochs.
    - Test of 60 images
    - 5 Mean of Dice for 104 classes
    - Draw the curves

# Experiment





# Proposed roadmap

The development process: From gathering requirements to launching a framework

# Roadmap

1. Identify annotations priorities
2. Set Goal for number of samples
3. Gather annotators (radiologists and oncologists)
4. Tools like 3D slicer and NORA
5. Active learning with a model trained on 4000+ samples
6. Intra and Inter reliability of annotators
7. Develop a Deep Learning framework
  - a. Based on MONAI
  - b. Inspired by nnU-Net
  - c. Modularity
8. Watch trends
  - a. Architectures innovations
  - b. Metrics innovations

# Roadmap

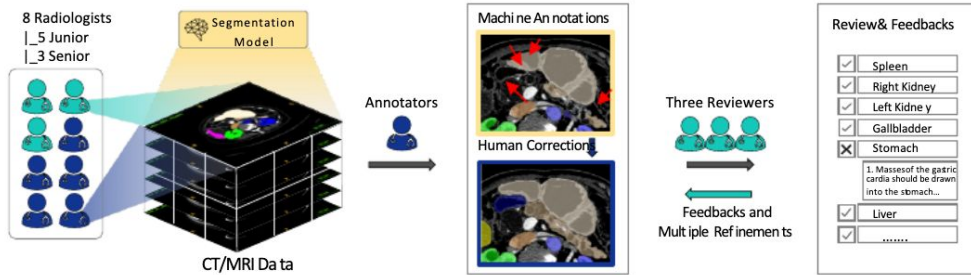


Figure 2: Annotation workflow of AMOS. The coarse annotations automatically labeled by pre-trained segmentors will be further refined by human annotators for multiple times, including 5 junior radiologists for the initial stage and 3 senior specialists for the second checking stage.

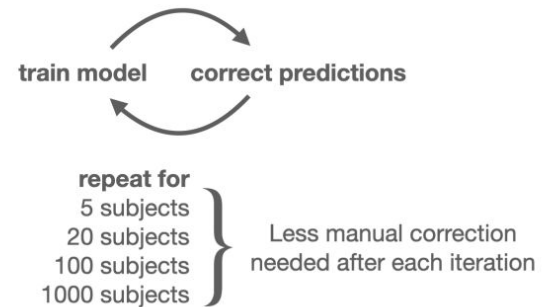
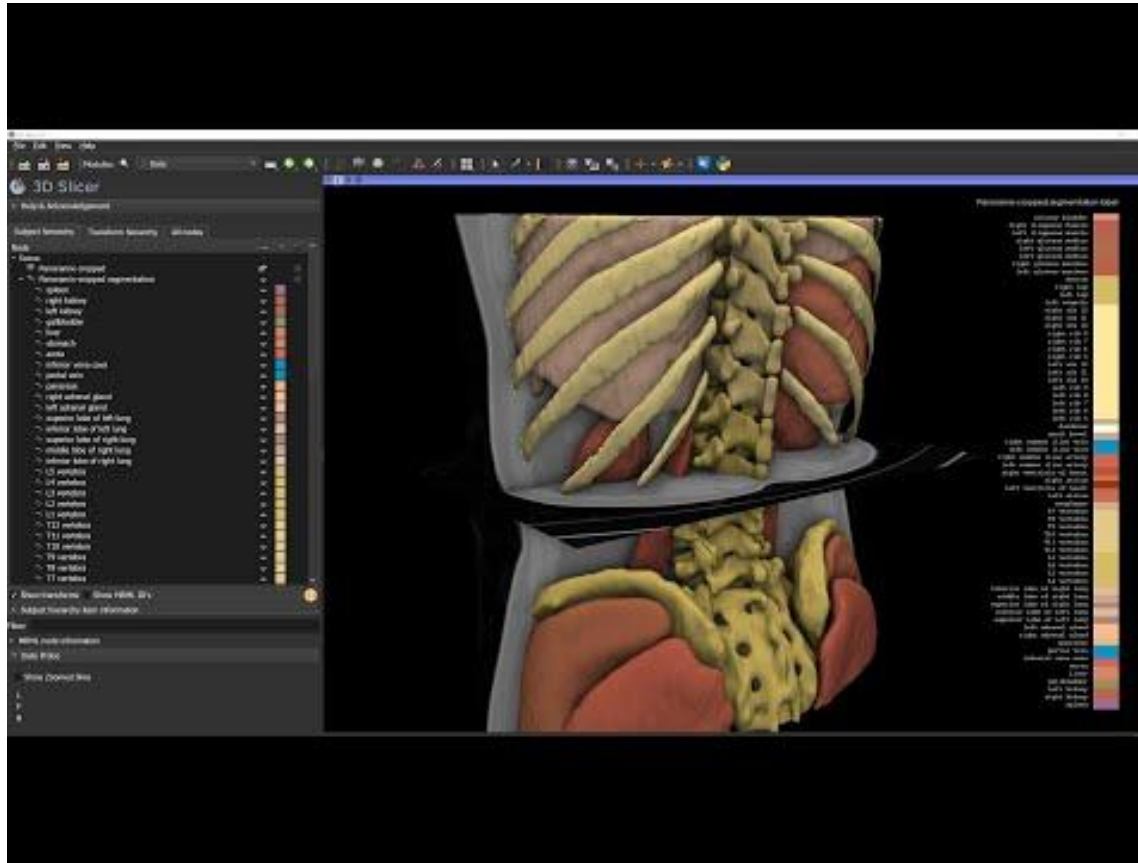


Figure 4. Overview of the active learning approach for manual segmentation: In a first step 5 subjects need to be labeled completely manually. Then a model is trained and only the model predictions are corrected. As soon as more data is labeled, the model is retrained, reducing the amount of manual corrections required.

# 3D slice and TotalSegmentator



# Conclusion

- Large and diverse database
- SOTA is nnU-Net
- Existing collaborations
- Learning curve experiment
- Roadmap based on the use of tools (3D slicer) and methods (Active learning), frameworks and trends watch.

# Litterature recommendation

nnUnet

AIMOS

Deepmind

TotalSegmentor

SwinUNETR

Pitfalls of image analysis metrics

Physician



DV.Target

